Appl Microbiol Biotechnol
DOI 10.1007/s00253-015-7025-z

Deletion of a gene cluster for [Ni-Fe] hydrogenase maturation in the anaerobic hyperthermophilic bacterium *Caldicellulosiruptor bescii* identifies its role in hydrogen metabolism

Minseok Cha[1,2] · **Daehwan Chung**[1,2] · **Janet Westpheling**[1,2]

Received: 9 July 2015 / Revised: 13 September 2015 / Accepted: 20 September 2015

Abstract The anaerobic, hyperthermophlic, cellulolytic bacterium *Caldicellulosiruptor bescii* grows optimally at ~80 °C and effectively degrades plant biomass without conventional pretreatment. It utilizes a variety of carbohydrate carbon sources, including both C5 and C6 sugars, released from plant biomass and produces lactate, acetate, CO_2, and H_2 as primary fermentation products. The *C. bescii* genome encodes two hydrogenases, a bifurcating [Fe-Fe] hydrogenase and a [Ni-Fe] hydrogenase. The [Ni-Fe] hydrogenase is the most widely distributed in nature and is predicted to catalyze hydrogen production and to pump protons across the cellular membrane creating proton motive force. Hydrogenases are the key enzymes in hydrogen metabolism and their crystal structure reveals complexity in the organization of their prosthetic groups suggesting extensive maturation of the primary protein. Here, we report the deletion of a cluster of genes, *hypABFCDE*, required for maturation of the [Ni-Fe] hydrogenase. These proteins are specific for the hydrogenases they modify and are required for hydrogenase activity. The deletion strain grew more slowly than the wild type or the parent strain and produced slightly less hydrogen overall, but more hydrogen per mole of cellobiose. Acetate yield per mole of cellobiose was increased ~67 % and ethanol yield per mole of cellobiose was decreased ~39 %. These data suggest that the primary role of the [Ni-Fe] hydrogenase is to generate a proton gradient in the membrane driving ATP synthesis and is not the primary enzyme for hydrogen catalysis. In its absence, ATP is generated from increased acetate production resulting in more hydrogen produced per mole of cellobiose.

Keywords Anaerobe · Hyperthermophile · *Caldicellulosiruptor bescii* · Hydrogen · Bifurcating [Fe-Fe] hydrogenase · [Ni-Fe] hydrogenase · Hydrogenase maturation proteins

Introduction

Caldicellulosiruptor bescii uses a variety of carbohydrates, including the simultaneous use of C5 and C6 sugars released from plant biomass. Glucose produced from these carbohydrates is oxidized through the Embden–Meyerhof–Parnas pathway (Fig. 1) producing acetate, lactate, CO_2, and hydrogen as major fermentative products (Chou et al. 2008; Schut and Adams 2009; Yang et al. 2009). In this pathway, carbon is directed to lactate or acetyl-CoA and electrons are directed to lactate and H_2 from pyruvate, which is a major metabolic branch point (Fig. 1) (Chou et al. 2008; Schut and Adams 2009; Yang et al. 2009). *Caldicellulosiruptor* spp. produce relatively high yields of H_2 (4 mol of H_2 per 1 mol of glucose) (de Vrije et al. 2007; Kadar et al. 2004; Kanai et al. 2005; Schicho et al. 1993; Willquist et al. 2010), and the generation of H_2 is coupled with the production of acetate and the electron carriers, NADH (a two electron carrier) and ferredoxin (a one electron carrier) (White 2007). Hydrogenases are used for proton reduction and H_2 formation (de Vrije et al. 2007; Kadar et al. 2004; Kanai et al. 2005; Schicho et al. 1993; Willquist et al. 2010). They are metalloenzymes classified by the metal content in the active site and fall into two groups, [Fe-Fe] and

Electronic supplementary material The online version of this article (doi:10.1007/s00253-015-7025-z) contains supplementary material, which is available to authorized users.

✉ Janet Westpheling
janwest@uga.edu

[1] Department of Genetics, University of Georgia, Athens, GA 30602, USA

[2] The BioEnergy Science Center, Oak Ridge National Laboratory, Oak Ridge, TN 37831, USA

Published online: 04 November 2015

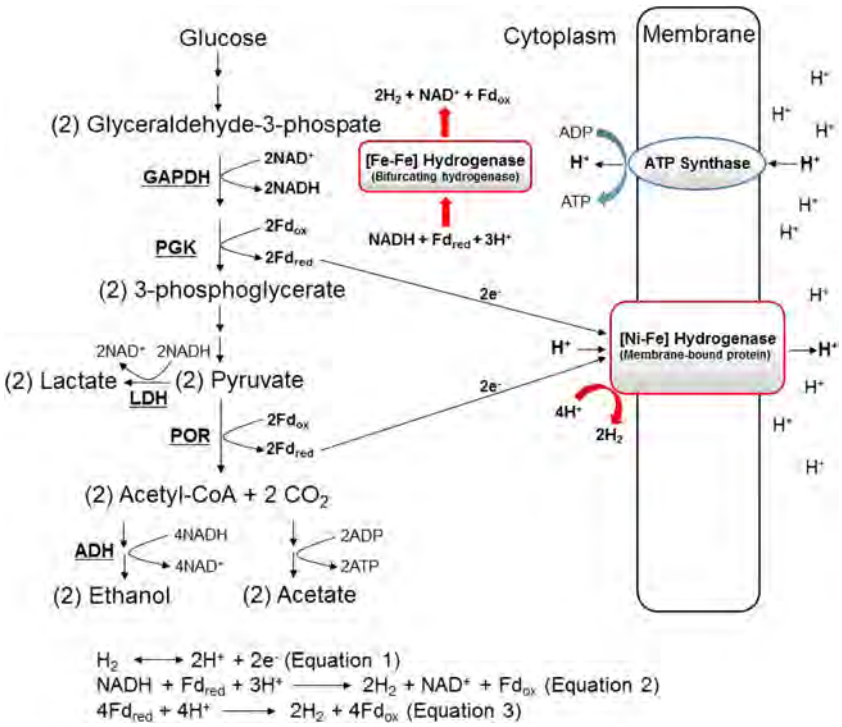

Fig. 1 Proposed metabolic pathways in *Caldicellulosiruptor bescii*. *GAPDH* glyceraldehyde 3-phosphate dehydrogenase, *PGK* phosphoglycerate kinase, *LDH* lactate dehydrogenase, *POR* pyruvate ferredoxin oxidoreductase, *ADH* bifunctional acetaldehyde/alcohol dehydrogenase, Fd_{red} reduced ferredoxin, Fd_{ox} oxidized ferredoxin

[Ni-Fe] hydrogenases (Casalot and Rousset 2001; Schicho et al. 1993; van de Werken et al. 2008), that provide a redox mechanism for storing and utilizing energy produced in the reaction (Fig. 1 (Equation 1)) (Schicho et al. 1993). *C. bescii* contains both types of hydrogenase, a cytoplasmic bifurcating [Fe-Fe] hydrogenase that requires NADH/NADPH and ferredoxin, simultaneously oxidized in a 1:1 stoichiometry to catalyze H_2 production (Carere et al. 2012; Schuchmann and Muller 2012; van de Werken et al. 2008) (the general overall reaction of the bifurcating hydrogenase is described in Fig. 1 (Equation 2)) and a [Ni-Fe] hydrogenase, a membrane bound heteromeric enzyme that is the most widely distributed hydrogenase in nature (Carere et al. 2012; Casalot and Rousset 2001; van de Werken et al. 2008). This enzyme only uses reduced ferredoxins as electron donors (Carere et al. 2012) (Fig. 1 (Equation 3)). The bifurcating [Fe-Fe] hydrogenase is likely to be the primary enzyme for the catalysis of H_2 production in *C. bescii*, and in addition to producing hydrogen, the [Ni-Fe] hydrogenase plays an important role in pumping out protons across the cellular membrane, thereby generating proton motive force (van de Werken et al. 2008) and ultimately ATP synthesis by chemiosmosis (Carere et al. 2012; Chou et al. 2008; van de Werken et al. 2008) (Fig. 1).

We recently engineered *C. bescii*, which does not produce ethanol naturally, for the direct conversion of switchgrass to ethanol by eliminating lactate dehydrogenase and inserting a bifunctional acetaldehyde/alcohol dehydrogenase from *Clostridium thermocellum* (Chung et al. 2014). While the yield of ethanol, greater than 60 % of theoretical based on substrate consumed, was surprisingly high, the titers were low and more work is needed to make *C. bescii* a viable candidate for consolidated bioprocessing on an industrial scale (Chung et al. 2014). Relatively little is understood about the primary metabolic pathways for carbon and electron flow in these thermophilic anaerobes and greater understanding of these pathways is essential for further engineering of fuels and bio-based products. Hydrogen production provides an essential release or "safety valve" (Casalot and Rousset 2001) for anaerobic bacteria that respire as electrons are redirected to electron acceptors when they become available.

Hydrogenase genes are often misannotated because of their similarity to dehydrogenase genes and are sometimes difficult to identify from genome sequence. The maturation proteins, required to produce active [Ni-Fe] hydrogenase, however, are easier to identify and are specific and absolutely required for the activity of the [Ni-Fe] hydrogenases (Casalot and Rousset 2001). To investigate the role of the *C. bescii* [Ni-Fe] hydrogenase in hydrogen production and cellular metabolism, we deleted a cluster of genes, *hypABFCDE*, involved in the maturation of the [Ni-Fe] hydrogenase in the ethanol-producing strain, an *ldh* deletion mutant with the engineered *adhE* gene present. The *C. bescii* wild-type and mutant strains were compared to assess lactate, acetate, and ethanol production by high-performance liquid chromatography (HPLC) and hydrogen production

by gas chromatography (GC). The mutant strain containing a deletion of the maturation gene cluster grew more slowly than the wild type suggesting that the [Ni-Fe] hydrogenase does, in fact, participate in metabolism as a proton pump to drive ATP synthesis. Deletion of the maturation gene cluster had little effect on hydrogen production overall, suggesting that the bifurcating [Fe-Fe] hydrogenase is likely the primary enzyme for hydrogen production in *C. bescii*. Carbon balance of the fermentation products from the wild-type, parent strain and *hypABFCDE* deletion strain suggested a redirection of carbon and electron flow in the mutant. These results provide important information for the continued metabolic engineering of these and similar microorganisms for the production of biofuels and bioproducts.

Materials and methods

Strains, media, and culture conditions

C. bescii strains and plasmids used in this study are shown in Table 1. All primers used are listed in Table S1. *C. bescii* strains were grown anaerobically in liquid or on solid surface in low osmolarity defined (LOD) medium (Farkas et al. 2013), final pH 7.0, with cellobiose (1.0 % *w*/*v*; Sigma-Aldrich, St. Louis, MO) as the carbon source unless otherwise noted. Liquid cultures were grown from a 1.0 % (*v*/*v*) inoculum or a single colony and incubated at 65 °C in anaerobic culture bottles degassed with five cycles of vacuum and argon. For growth of uracil auxotrophic mutants, the LOD medium was supplemented with 1.0 mM uracil. *Escherichia coli* DH5α was used for plasmid DNA constructions and preparations. Standard techniques for *E. coli* were performed as described (Green et al. 2012). *E. coli* cells were grown in Luria Bertani (LB) broth supplemented with apramycin (50 μg/ml), and plasmid DNA was isolated using a Qiagen Mini-prep Kit (Qiagen, Valencia, CA). Chromosomal DNA from *C. bescii* strains was extracted using the Quick-gDNA™ MiniPrep (Zymo Research Corp., Irvine, CA) or using the DNeasy Blood & Tissue Kit (Qiagen, Valencia, CA) according to the manufacturer's instructions. All strains are available upon request.

Construction of pDCW158

All PCR reactions described in this study used high fidelity *pfu* AD DNA polymerase (Agilent Tech., Santa Clara, CA). PCR reactions, restriction enzyme digests (NEB, Ipswich, MA), and the Fast-link DNA Ligase kit (Epicentre, Madison, WI) were used according to the manufacturer's instructions. For the construction of a plasmid for the deletion of the [Ni-Fe] hydrogenase maturation gene cluster (*hypABFCDE*; Cbes1088~Cbes1093), three cloning steps including overlapping polymerase chain reactions were performed. A 1-kb fragment upstream of the *hypABFCDE* cluster was amplified with primers DC516 that contained a *Bam*HI site and DC517 that was also used for overlapping PCR amplification. A 1-kb fragment, downstream of the *hypABFCDE*, was amplified with primer DC518 (used for overlapping PCR amplification) and primer DC519 that contained an *Apa*LI site. The two fragments were joined using primers DC516 and DC519 to generate a 2-kb product that was cloned into pDCW088 (Chung et al. 2013b) using the *Bam*HI and *Apa*LI sites. The details of pDCW158 are described in Fig. 2 (A) and Figure S2. The resulting plasmid, pDCW158, was transformed into *E. coli* DH5α by electrotransformation via a single electric pulse (1.8 kV, 25 μF, and 200 Ω) in a pre-chilled 1-mm cuvette using a Bio-Rad gene Pulser (Bio-Rad, Hercules, CA). *E. coli* transformants were selected on LB solid medium containing apramycin (50 μg/ml final concentration). pDCW158

Table 1 *C. bescii* strains and plasmids used in this study

Strains/plasmids	Strain and genotype/phenotype	Source
Wild type	*C. bescii* DSMZ6725 wild type/(*ura*$^{+}$/5-FOA^{S})	DSMZ[a]
JWCB017	*ΔpyrFA Δldh*/(*ura*$^{-}$/5-FOA^{R})	(Cha et al. 2013)
JWCB036	*ΔpyrFA Δldh CIS1*::P$_{S\text{-}layer}$ *Cthe-adhE*/(*ura*$^{-}$/5-FOA^{R})	This study
JWCB038	*ΔpyrFA Δldh CIS1*::P$_{S\text{-}layer}$ *Cthe-adhE ΔhypADFCDE*/(*ura*$^{-}$/5-FOA^{R})	This study
pDCW088	*cbeI* deletion vector (Apramycin^{R})	(Chung et al. 2013b)
pDCW144	Integrational vector containing the P$_{S\text{-}layer}$ *Cthe-adhE*[b]	(Chung et al. 2014)
pDCW158	*hypABFCDE*[c] deletion vector (Apramycin^{R})	This study

[a] German Collection of Microorganisms and Cell Cultures

[b] *Cthe-adhE* (Cthe0423; Bifunctional acetaldehyde/alcohol dehydrogenase derived from *Clostridium thermocellum* ATCC27405)

[c] *hypABFCDE* (Cbes1088~Cbes1093; [Ni-Fe] hydrogenase maturation protein genes)

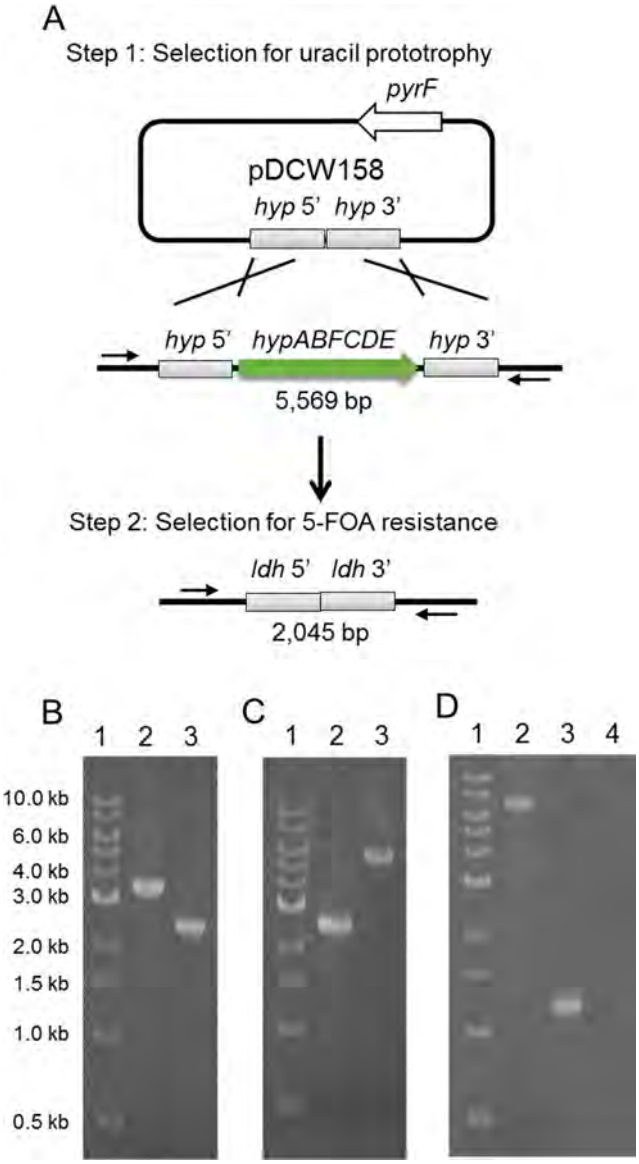

Fig. 2 Targeted deletion of *hypABFCDE* in *C. bescii*. (*A*) A deletion of the *hyp* gene cluster was constructed in a non-replicating plasmid that contained a wild-type copy of the *pyrF* gene (pDCW158). The plasmid contained the DNA sequence 5′ and 3′ flanking the cluster. Uracil prototrophy selected targeted integration of the plasmid into the *hyp* locus in JWCB036 (*ΔpyrFA Δldh CIS1*::$P_{S\text{-}layer}$ *Cthe-adhE*). Counter-selection with 5-FOA selected plasmid loss and resistant colonies were screened for deletion of the *hypABFCDE* cluster, resulting in strain JWCB038 (*ΔpyrFA Δldh CIS1*::$P_{S\text{-}layer}$ *Cthe-adhE ΔhypADFCDE*). (*B*) A gel depicting PCR products amplified from the *ldh* locus from the wild-type (3.3 kb product, *lane 2*) and the *ldh* deletion strain (2.4 kb, *lane 3*). (*C*) PCR products amplified from the targeted chromosome region for the *C. thermocellum adhE* (Cthe0423) insertion from the wild-type (2.6 kb, *lane 2*) and the insertion strain (5.4 kb, *lane 3*). (*D*) PCR products amplified from the *hypABFCDE* locus in the wild-type (6.8 kb, *lane 2*) and the *ΔhypADFCDE* deletion strain (1.2 kb, *lane 3*). *Lane 1* in each gel, 1.0 kb DNA ladder; *lane 4* (*D*), no DNA control for the PCR reaction preformed for each reaction

was verified by DNA sequencing (Macrogen, Rockville, MD) and is available on request.

Preparation of competent cells, transformation, screening, purification, and sequence verification of engineered *C. bescii* mutants, JWCB036 and JWCB038

To prepare competent cells, 50-ml cultures were grown in LOD medium at 75 °C for 18 h (to mid exponential phase) and 25 ml of the culture was used to inoculate a 500-ml culture of LOD supplemented with a final concentration of 40 μM uracil and a mixture of 19 amino acids (5 % inoculum, *v*/*v*) (Farkas et al. 2013). The 500-ml culture was incubated at 75 °C for 5 h and cooled to room temperature for 1 h. Cells were harvested by centrifugation (6000×*g*, 20 min) at 25 °C, washed three times with 50 ml of pre-chilled 10 % sucrose and after the third wash, the cell pellet was resuspended in 50 μl of pre-chilled 10 % sucrose in a microcentrifuge tube and stored at −80 °C. Before transformation, plasmids from *E. coli* were methylated in vitro using *C. bescii* methyltransferase (M.*Cbe*I, (Chung et al. 2013a)). To construct strain JWCB036, 1 μg of methylated pDCW144 DNA was used to electrotransform JWCB017 (*ΔpyrFA Δldh*, (Cha et al. 2013)), and 1 μg of methylated pDCW158 DNA was used to electrotransform JWCB036 (*ΔpyrFA Δldh CIS1*::$P_{S\text{-}layer}$ *Cthe-adhE*) to construct the strain JWCB038 (*ΔpyrFA Δldh CIS1*::$P_{S\text{-}layer}$ *Cthe-adhE ΔhypABFCDE*) as described (Chung et al. 2013b). Electrotransformation of the cell/DNA mixture was performed via single electric pulse (1.8 kV, 25 μF, and 350 Ω) in a pre-chilled 1-mm cuvette using a Bio-Rad gene pulser (Bio-Rad, Hercules, CA). Cells were then plated onto solid LOD medium (without uracil), and uracil prototrophic transformant colonies were inoculated into liquid medium for genomic DNA extraction and subsequent PCR screening of the targeted region to confirm the integration of pDCW144 and pDCW158 into the chromosome. Confirmed transformants were inoculated into nonselective LOD medium with 1.0 mM uracil and incubated overnight at 65 °C, then plated onto 5-FOA (8 mM) containing solid medium. After initial screening, transformants were further purified by one additional passage of a single colony under selection on the solid medium and screened a second time by PCR to check for segregation of the $P_{S\text{-}layer}$-*adhE* insertion and deletion of *hypABFCDE*. The locations of insertions and deletions in the chromosome were verified by PCR amplification and DNA sequence analysis. A PCR product for the $P_{S\text{-}layer}$-*adhE* insertion was generated from genomic DNA using primers (DC477 and DC478) outside the homologous regions used to construct the integration and internal primers (DC456, DC457, DC462, and DC463). A PCR product for the deletion of *hypABFCDE* was generated from genomic DNA with primers MC012 and MC020.

Growth comparison of *C. bescii* mutants and HPLC ananlysis of fermentation products

Cells were grown in stoppered 125-ml serum bottles containing 50 ml LOD medium supplemented with 1 % (*w*/*v*) cellobiose (Sigma-Aldrich, St. Louis, MO) and 1 mM uracil. Duplicate bottles were inoculated with a fresh 1 % (*v*/*v*) inoculum and incubated at 65 °C with shaking at 150 rpm. Optical cell density was monitored using a Jenway Genova spectrophotometer (Jenway, Burlington, NJ) measuring absorbance at 680 nm. Batch fermentations were performed at 65 °C in the same culture conditions, except with 1 % (*w*/*v*) cellobiose, 2 % (*w*/*v*) Avicel (Sigma-Aldrich, St. Louis, MO), or 2 % (*w*/*v*) switchgrass. Prepared switchgrass (supplied by Brian Davison, Oak Ridge National Laboratory), (*Panicum virgatum*, Alamo variety) had been air-dried, reduced to 60 mesh using a Wiley Mini-Mill (Thomas Scientific, Swedesboro, NJ) and subjected to a hot water treatment similar to that described by Yang et al. 2009; however, the biomass was boiled in distilled H_2O (2 %; *w*/*v*) for 1 h rather than treating overnight at 75 °C. The switchgrass was then washed and dried overnight at 50 °C before dispensing into serum bottles as previously described (Yang et al. 2009). Cellobiose, glucose, acetate, lactate, and ethanol were monitored on an Agilent 1200 infinity high-performance liquid chromatography (HPLC) system (Agilent Tech., Santa Clara, CA). Metabolites were separated on an Aminex HPX-87 H column (Bio-Rad, Hercules, CA) under isocratic temperature (50 °C) at a flow of 0.6 ml/min in 5.0 mM H_2SO_4 then passed through a refractive index detector (Agilent 1200 Infinity Refractive Index Detector; Agilent Tech., Santa Clara, CA). Identification was performed by comparison of retention times with standards; cellobiose—7.12 min, glucose—8.71 min, lactate—12.31 min, acetate—14.64 min, and ethanol—20.99 min. The total peak areas were integrated and compared to peak areas and retention times of known standards for each compound of interest.

GC analysis for H_2 production

After 36 h incubation at 65 °C, the culture bottles were cooled to room temperature and H_2 was measured on a gas chromatography (GC) model 8610C (SRI Instruments, Menlo Park, CA) equipped with a thermal conductivity detector at 80 °C with a N_2 reference flow and a 1.83 m × 3.18 mm (inside diameter) stainless-steel column packed with Porapak-Q (80/100 mesh; SRI Instruments, Menlo Park, CA). Identification of the hydrogen peak was performed by comparison of retention times with H_2 standards. The total peak areas were integrated and compared to peak areas and retention times of known H_2 standards.

Results

Deletion of the [Ni-Fe] hydrogenase maturation gene cluster (*hypABFCDE*) from the *C. bescii* chromosome

We previously reported a method for DNA transformation and marker replacement in *C. bescii* based on uracil prototrophic selection (Chung et al. 2013a; Chung et al. 2012; Chung et al. 2013b) and reported the complete deletion of lactate dehydrogenase (*ldh*) using this method (Cha et al. 2013). The *ldh* deletion strain (JWCB017; *ΔpyrFA Δldh*) (Cha et al. 2013) was constructed in *C. bescii* JWCB005 (*ΔpyrFA*) (Cha et al. 2013; Chung et al. 2013a; Chung et al. 2013b), a uracil auxotroph resistant to 5-fluoroorotic acid (5-FOA) (Table 1). This strain produced more hydrogen and acetate and grew better than the wild-type strain, likely because of the increased ATP production derived from the production of additional acetate (Cha et al. 2013). The *adhE* gene (Cthe0423), from *Clostridium thermocellum*, that encodes a bifunctional acetaldehyde/alcohol dehydrogenase was inserted into the *C. bescii* JWCB017 chromosome as described (Chung et al. 2014) (Figure S1), and this strain, JWCB036 (*ΔpyrFA Δldh CIS1*::$P_{S\text{-}layer}$ *Cthe-adhE*), produced ethanol directly from switchgrass, as well as Avicel and cellobiose. A deletion of the [Ni-Fe] hydrogenase maturation gene cluster (*hypABFCDE*; Cbes1088~Cbes1093) was constructed in JWCB036 by fusing the 5′ and 3′ flanking regions of the *hypABFCDE* gene cluster and cloning the fused product into a non-replicating plasmid vector, resulting in plasmid pDCW158 (Fig. 2 (A) and Figure S2). This vector also contained the wild-type *pyrF* allele under the transcriptional control of a ribosomal protein gene promoter (Cbes2105, 30S ribosomal protein S30EA), allowing both positive (uracil prototrophy) and negative (5-FOA resistance) selection (Fig. 2 (A). Plasmid pDCW158 was transformed into *C. bescii* JWCB036 (*ΔpyrFA Δldh CIS1*::$P_{S\text{-}layer}$ *Cthe-adhE*) selecting uracil prototrophy resulting from plasmid recombination into the targeted region of the chromosome, followed by counter-selection with 5-FOA resulting from plasmid excision. The resulting strain, JWCB038 (*ΔpyrFA Δldh CIS1*::$P_{S\text{-}layer}$ *Cthe-adhE ΔhypABFCDE*), contained a deletion of the *hypABFCDE* gene cluster. To confirm the *ldh* and *hypABFCDE* deletions in this strain, the chromosomal regions of the *ldh* and *hypABFCDE* locus were amplified by PCR using primers outside the plasmid regions of homology used to construct the deletions. The *adhE* insertion was confirmed using primers to amplify the targeted region of the chromosome containing the insertion. PCR amplification of DNA from JWCB038 shown in Fig. 2 (B), using the wild-type strain as a control, provides evidence that JWCB038 contains a deletion of the *ldh* gene, (the wild-type strain shows a 3.3-kb product, while PCR from JWCB038 (*ΔpyrFA Δldh CIS1*::$P_{S\text{-}layer}$ *Cthe-adhE ΔhypABFCDE*) resulted in a 2.4-kb product.

Evidence that JWCB038 contains an insertion of the *adhE* gene is provided by amplification of the *adhE* cassette from the wild type which generates a 2.6-kb product and JWCB038 resulting in a 5.4-kb product (Fig. 2 (C). Evidence for the deletion of *hypABFCDE* in JWCB038 comes from amplification of this region of the chromosome from the wild type, which show 6.7-kb products compared to a 1.2-kb product from JWCB038 (Fig. 2 (D).

Comparison of growth yields and hydrogen production in the wild-type and *hypABFCDE* deletion strain

Growth of the mutant strains, JWCB017 (*ΔpyrFA Δldh*), JWCB036 (*ΔpyrFA Δldh CIS1*::$P_{S\text{-}layer}$ *Cthe-adhE*), and JWCB038 (*ΔpyrFA Δldh CIS1*::$P_{S\text{-}layer}$ *Cthe-adhE ΔhypABFCDE*), was compared to the wild-type strain in a low osmolarity defined (LOD) medium (Farkas et al. 2013) supplemented with 1.0 % cellobiose (w/v) as carbon source (Fig. 3a). The doubling time for all four strains was ~2.2 h. Although the doubling time was similar, the maximum $OD_{680\ nm}$ of the *hypABFCDE* deletion strain, JWCB038, was ~20 % lower than the others (Fig. 3a) and showed a longer lag phase suggesting that [Ni-Fe] hydrogenase may participate in energy production likely as a proton pump to generate proton motive force in the membrane to drive ATP synthesis.

To compare hydrogen production, the *C. bescii* wild-type and mutant strains were grown in LOD medium (Farkas et al. 2013) with 1 % cellobiose (*w/v*), 2 % Avicel (*w/v*) or 2 % switchgrass (*w/v*) as carbon source (Fig. 3B). NADH accumulates in the *ldh* deletion strain (JWCB017), and the accumulated NADH is presumably used for the catalysis of H_2 production. In fact, this deletion resulted in 30 ~ 40 % more H_2 production compared to the wild-type strain (Fig. 3B). On the other hand, the strain containing the *adhE* gene (JWCB036), showed about 20–50 % less H_2 production than the wild-type (Fig. 3B) presumably because JWCB036 produces ethanol and the ethanol production pathway draws NADH from the H_2 production pathway, reducing H_2 production. Deletion of the *hypABFCDE* gene cluster in JWCB038 resulted slower growth and a ~ 20 % reduction in H_2 production compared to the JWCB036 parent strain (Fig. 3A and B). As shown in Table S2, however, the hydrogen yield per mole of cellobiose was increased to ~63 % in JWCB038 compared to that in the parent stain.

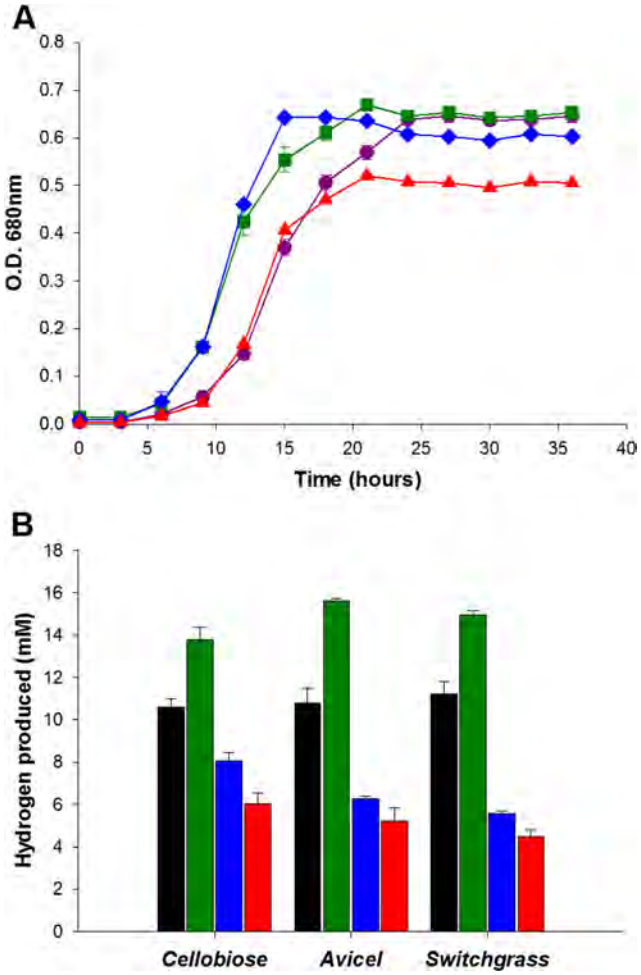

Fig. 3 Comparison of growth ($OD_{680\ nm}$) and hydrogen production for the wild-type and *ΔhypADFCDE* mutant strains. **a** Growth of *C. bescii* strains on 1 % cellobiose as a sole carbon source; *black circles*, wild-type; *green squares*, JWCB017 (*ΔpyrFA Δldh*); *blue diamonds*, JWCB036 (*ΔpyrFA Δldh CIS1*::$P_{S\text{-}layer}$ *Cthe-adhE*); *red triangles*, JWCB038 (*ΔpyrFA Δldh CIS1*::$P_{S\text{-}layer}$ *Cthe-adhE ΔhypADFCDE*). **b** Hydrogen produced by each strain at the end of incubation (36 h); *black bars*, wild-type; *green bars*, JWCB017; *blue bars*, JWCB036; *red bars*, JWCB038. *Error bars* based on two biologically independent experiments.

Analysis of the fermentation products of the *hypABFCDE* deletion strain on different carbon sources and carbon balances

To investigate possible changes in carbon flow during fermentation in the *hypABFCDE* deletion strain, *C. bescii* wild-type and mutant strains were grown in LOD medium (Farkas et al. 2013) with 1 % (*w/v*) cellobiose, 2 % (*w/v*) Avicel, or 2 % (*w/v*) switchgrass as carbon source and the production of lactate, acetate, and ethanol was compared. The fermentation products were monitored over the course of 36 h by HPLC analysis (Fig. 4), and final carbon utilization was calculated (Fig. 5 and Table S2). At 36 h, HPLC analysis of *C. bescii* wild type showed the production of lactate (1.2 mM from cellobiose, 3.1 mM from avicel, 2.7 mM from switchgrass), acetate (7.1 from cellobiose, 5.5 from avicel, and 7.9 mM from switchgrass), and no ethanol (Fig. 4). The *ldh* deletion strain, JWCB017, did not produce lactate or ethanol but did produce more acetate (9.2 mM on cellobiose, 7.4 mM on avicel, and 9.5 mM on switchgrass). The increased acetate production in the *ldh* deletion strain compared to the wild type suggests increased carbon flow to acetate (Fig. 4). The strain

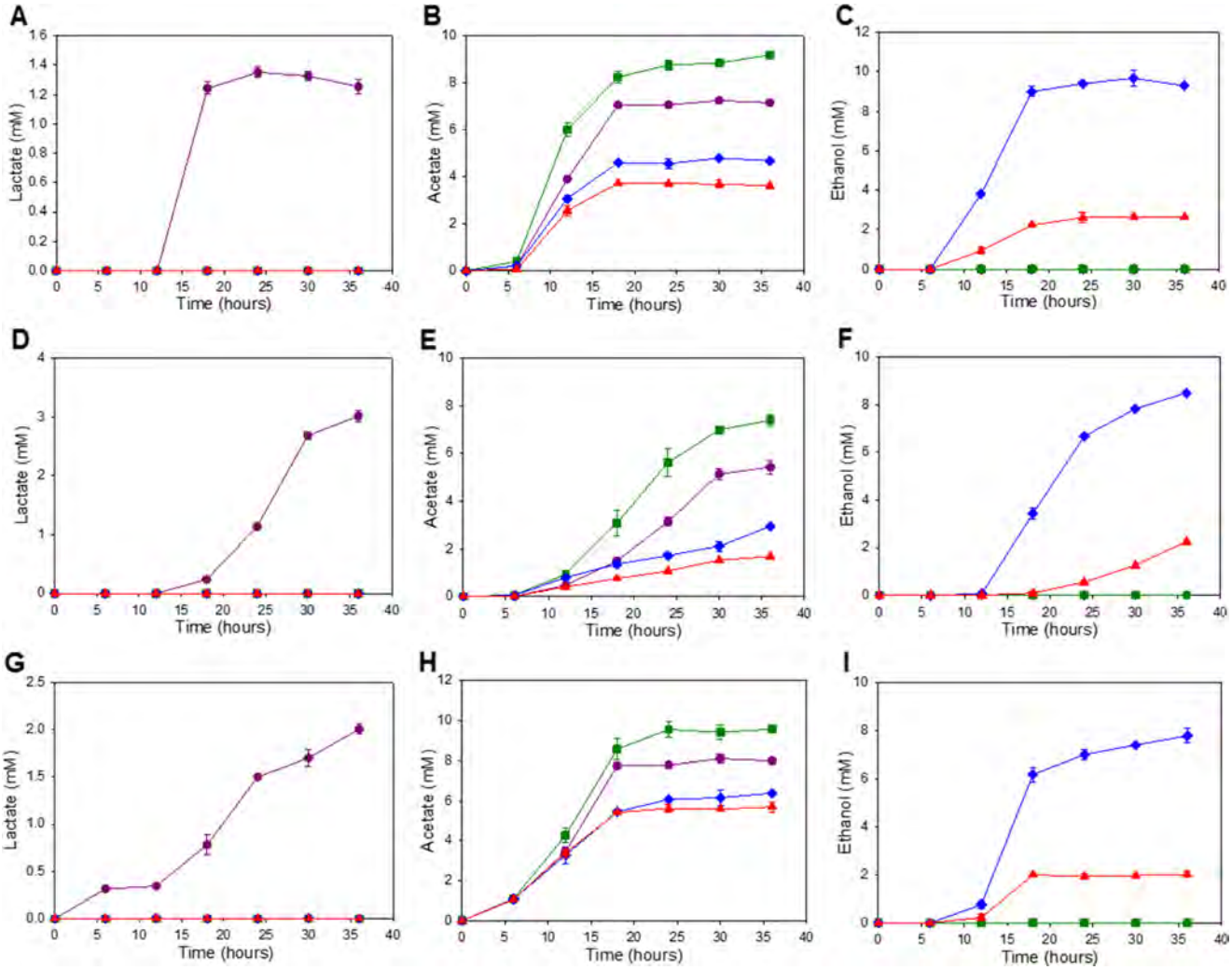

Fig. 4 Comparison of fermentation products by *C. bescii* mutant strains. Analysis of fermentation products lactate (**a**, **d**, **g**), acetate (**b**, **e**, **h**), and ethanol (**c**, **f**, **i**) grown on 1 % (w/v) cellobiose (**a**, **b**, **c**), 2 % (w/v) Avicel (**d**, **e**, **f**), and 2 % (w/v) switchgrass (**g**, **h**, **i**) at 65 °C; *dark pink circles*, wild-type; *green squares*, JWCB017 (*ΔpyrFA Δldh*); *blue diamonds*, JWCB036 (*ΔpyrFA Δldh CIS1*::$P_{S\text{-}layer}$ *Cthe-adhE*); *red triangles*, JWCB038 (*ΔpyrFA Δldh CIS1*::$P_{S\text{-}layer}$ *Cthe-adhE ΔhypADFCDE*). *Error bars* based on two biologically independent experiments.

engineered to produce ethanol, JWCB036, produced ethanol (9.2 mM from cellobiose, 8.5 mM from avicel, and 9.7 mM from switchgrass), but no lactate and less acetate (4.6 mM from cellobiose, 3.0 mM, from avicel, 6.3 mM from switchgrass) indicating redirection of carbon from pyruvate to acetate and increased carbon to ethanol production (Fig. 4). The *hypABFCDE* deletion strain, JWCB038, produced acetate (3.6 mM from cellobiose, 1.6 mM from avicel, 5.7 mM from switchgrass) and ethanol (2.7 mM from cellobiose, 2.2 mM from avicel, 1.9 mM from switchgrass). The reduction in acetate (34 %) and ethanol (73 %) compared to the parent strain, JWCB036, likely resulted from reduced growth of this strain.

The carbon mass balance for end products from 1 % cellobiose was measured by HPLC and calculated at 36 h (Fig. 5 and Table S2). The wild type showed 1 % conversion of cellobiose to lactate (1.3 mM) and 5.4 % to acetate (7.1 mM), with 96 % carbon recovery overall. This strain produced no ethanol. The *ldh* deletion mutant, JWCB017, produced no lactate and showed 6.5 % conversion of cellobiose to acetate (9.2 mM) with 105 % overall carbon recovery. The engineered ethanol strain, JWCB036, produced no lactate, 3.7 % conversion of cellobiose to acetate (4.7 mM) and 7.2 % to ethanol (9.3 mM) with an overall 95 % carbon recovery. The *hypABFCDE* deletion strain, JWCB038, produced no lactate, 3 % conversion of cellobiose to acetate (3.6 mM) and 2.2 % to ethanol (2.6 mM) with 94 % carbon recovery overall (Fig. 5a and Table S2).

Discussion

Hydrogenases play an important role in microbial energy metabolism, but the nature and function of these enzymes is not completely understood (Vignais and Colbeau 2004). In this

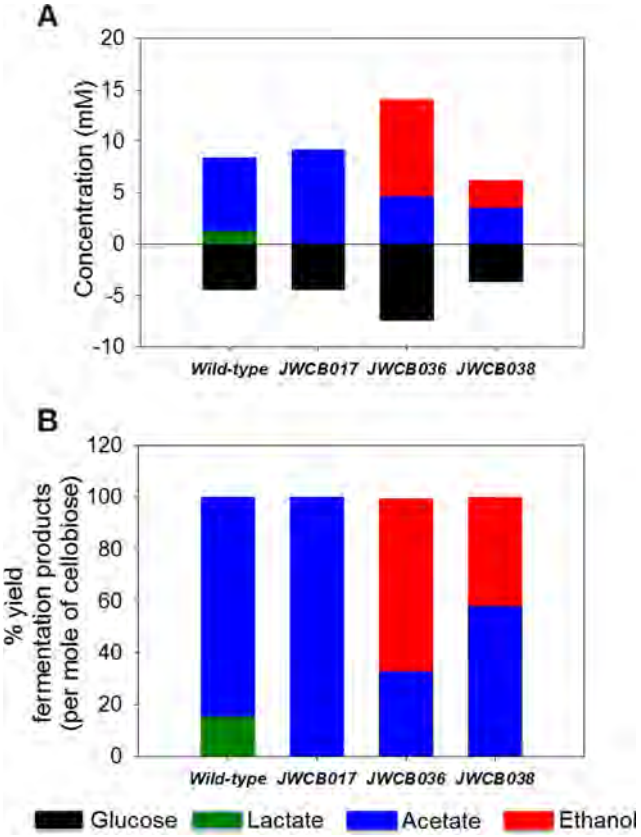

Fig. 5 Carbon balance of fermentation products of *C. bescii* mutant strains. **a** Concentrations of fermentation products from catabolized glucose equivalents. **b** % yields of final fermentation products per mole of cellobiose; *black bars*, glucose; green bars, lactate; *blue bars*, acetate; red bars, ethanol

study, we report the deletion of a gene cluster, *hypABFCDE*, that encodes the maturation proteins for the *C. bescii* [Ni-Fe] hydrogenase. The resulting strain, JWCB38 (*ΔpyrFA Δldh CIS1*::$P_{S\text{-}layer}$ *Cthe-adhE ΔhypABFCDE*), grew less well than the wild-type or parent strain suggesting that the primary function of this enzyme, like others in its class (Chou et al. 2008; Das et al. 2006), is to act as a proton pump generating proton motive force in the cellular membrane contributing to ATP synthesis (Fig. 1) (Chou et al. 2008; White 2007). There was no significant reduction in overall hydrogen production in the deletion strain suggesting that the [Ni-Fe] hydrogenase is not the primary enzyme in *C. bescii* for hydrogen production and that this function is likely provided by the bifurcating [Fe-Fe] hydrogenase. *Clostridium pasteurianum*, for example, contains both a [Fe-Fe] and [Ni-Fe] hydrogenase that are active in hydrogen production in fermentation, but the [Fe-Fe] hydrogenase is the primary hydrogen-producing enzyme (Cammack 1999). There was, however, a significant effect on carbon flux in this strain as well as the apparent availability of the cofactor NADH. In fact, the deletion strain produced more hydrogen per mole of cellobiose than the engineered ethanol-producing parent strain. Conversion of 1 mol cellobiose to pyruvate via the EMP pathway produces 4 mol of ATP and 4 mol of reducing equivalents in the form of NADH. When pyruvate is converted to ethanol, 2 mol of NADH are oxidized to NAD+. Pyruvate to acetate produces 1 mol of ATP and NADH is not oxidized. The conversion of cellobiose to acetate, therefore, has the advantage in that in a redox balanced pathway, 1 net ATP is produced. The *hypACFCDE* deletion strain, JWCB038, produced ~39 % less ethanol and ~67 % more acetate per mole of cellobiose compared to the parental strain (JWCB036) (Fig. 5b and Table S2). We speculate that to compensate for the loss of the proton pump, and therefore loss of ATP production in the *hypABFCDE* deletion strain, the cells apparently shift carbon flow to acetate to produce more ATP. This kind of shift in carbon flux in the deletion strain should also affect the NAD^+/NADH ratio in the fermentation process, increasing the availability of NADH. The reducing power stored in NADH can then be used by the bifurcating [Fe-Fe] hydrogenases (Fig. 1 (Equation 2)), as evidenced by the ~63 % increased in hydrogen produced per mole of catabolized cellobiose compared to the parent strain (Table S2). This analysis is the first deletion of a hydrogenase in this genus and provides some insight into the metabolic pathways in *C. bescii*. [Ni-Fe] hydrogenases are classified in to four major groups: (1) hydrogen uptake hydrogenases, (2) cytoplasmic H_2 sensors such as the cyanbacterial uptake [Ni-Fe] hydrogenases, (3) bidirectional heteromultimeric cytoplasmic [Ni-Fe] hydrogenases, and (4) H_2-evolving energy-conserving membrane-associated hydrogenases. This study clearly suggests that the [Ni-Fe] hydrogenase in *C. bescii* falls into group 4, the H_2-evolving energy-conserving membrane-associated hydrogenases (Vignais and Colbeau 2004). Very little is known about the regulation of carbon and electron flow in these bacteria, and this work will contribute to a basic understanding of these processes as well as further metabolic engineering for the production of biofuels and bioproducts.

Acknowledgments We thank Jennifer Copeland and Elise Snyder for the outstanding technical assistance, Brian Davison for providing the switchgrass used in this study, Sidney Kushner for the expert technical advice, William Whitman for the advice and use of his GC, Joe Groom and Jenna Young for the critical review of the manuscript. The BioEnergy Science Center is a U.S. Department of Energy Bioenergy Research Center supported by the Office of Biological and Environmental Research in the DOE Office of Science.

Compliance with ethical standards

Conflict of interest The authors declare that they have no competing interests.

References

Cammack R (1999) Hydrogenase sophistication. Nature 397(6716):214–215. doi:10.1038/16601

Carere CR, Rydzak T, Verbeke TJ, Cicek N, Levin DB, Sparling R (2012) Linking genome content to biofuel production yields: a meta-analysis of major catabolic pathways among select H_2 and ethanol-producing bacteria. BMC Microbiol 12:295. doi:10.1186/1471-2180-12-295

Casalot L, Rousset M (2001) Maturation of the [NiFe] hydrogenases. Trends Microbiol 9:228–237

Cha M, Chung D, Elkins JG, Guss AM, Westpheling J (2013) Metabolic engineering of *Caldicellulosiruptor bescii* yields increased hydrogen production from lignocellulosic biomass. Biotechnol Biofuels 6(1):85. doi:10.1186/1754-6834-6-85

Chou CJ, Jenney Jr FE, Adams MW, Kelly RM (2008) Hydrogenesis in hyperthermophilic microorganisms: implications for biofuels. Metab Eng 10(6):394–404. doi:10.1016/j.ymben.2008.06.007

Chung D, Cha M, Farkas J, Westpheling J (2013a) Construction of a stable replicating shuttle vector for *Caldicellulosiruptor* species: use for extending genetic methodologies to other members of this genus. PLoS One 8(5):e62881. doi:10.1371/journal.pone.0062881

Chung D, Cha M, Guss AM, Westpheling J (2014) Direct conversion of plant biomass to ethanol by engineered *Caldicellulosiruptor bescii*. Proc Natl Acad Sci U S A 111(24):8931–8936. doi:10.1073/pnas.1402210111

Chung D, Farkas J, Huddleston JR, Olivar E, Westpheling J (2012) Methylation by a unique alpha-class N4-cytosine methyltransferase is required for DNA transformation of *Caldicellulosiruptor bescii* DSM6725. PLoS One 7(8):e43844. doi:10.1371/journal.pone.0043844

Chung D, Farkas J, Westpheling J (2013b) Overcoming restriction as a barrier to DNA transformation in *Caldicellulosiruptor* species results in efficient marker replacement. Biotechnol Biofuels 6(1):82. doi:10.1186/1754-6834-6-82

Das D, Dutta T, Nath K, Kotya SM, Das AK, Veziroglu TN (2006) Role of hydrogenase in biological hydrogen production. Curr Sci 90(12):1627–1637

de Vrije T, Mars AE, Budde MA, Lai MH, Dijkema C, de Waard P, Claassen PA (2007) Glycolytic pathway and hydrogen yield studies of the extreme thermophile *Caldicellulosiruptor saccharolyticus*. Appl Microbiol Biotechnol 74(6):1358–1367. doi:10.1007/s00253-006-0783-x

Farkas J, Chung D, Cha M, Copeland J, Grayeski P, Westpheling J (2013) Improved growth media and culture techniques for genetic analysis and assessment of biomass utilization by *Caldicellulosiruptor bescii*. J Ind Microbiol Biotechnol 40(1):41–49. doi:10.1007/s10295-012-1202-1

Green MR, Sambrook J, Sambrook J (2012) Molecular cloning : a laboratory manual, 4th edn. Cold Spring Harbor Laboratory Press, Cold Spring Harbor

Kadar Z, de Vrije T, van Noorden GE, Budde MA, Szengyel Z, Reczey K, Claassen PA (2004) Yields from glucose, xylose, and paper sludge hydrolysate during hydrogen production by the extreme thermophile *Caldicellulosiruptor saccharolyticus*. Appl Biochem Biotechnol 113-116:497–508

Kanai T, Imanaka H, Nakajima A, Uwamori K, Omori Y, Fukui T, Atomi H, Imanaka T (2005) Continuous hydrogen production by the hyperthermophilic archaeon, *Thermococcus kodakaraensis* KOD1. J Biotechnol 116(3):271–282. doi:10.1016/j.jbiotec.2004.11.002

Schicho RN, Ma K, Adams MW, Kelly RM (1993) Bioenergetics of sulfur reduction in the hyperthermophilic archaeon *Pyrococcus furiosus*. J Bacteriol 175(6):1823–1830

Schuchmann K, Muller V (2012) A bacterial electron-bifurcating hydrogenase. J Biol Chem 287(37):31165–31171. doi:10.1074/jbc.M112.395038

Schut GJ, Adams MW (2009) The iron-hydrogenase of *Thermotoga maritima* utilizes ferredoxin and NADH synergistically: a new perspective on anaerobic hydrogen production. J Bacteriol 191(13):4451–4457. doi:10.1128/JB.01582-08

van de Werken HJ, Verhaart MR, VanFossen AL, Willquist K, Lewis DL, Nichols JD, Goorissen HP, Mongodin EF, Nelson KE, Van Niel EW, Stams AJ, Ward DE, de Vos WM, van der Oost J, Kelly RM, Kengen SW (2008) Hydrogenomics of the extremely thermophilic bacterium *Caldicellulosiruptor saccharolyticus*. Appl Environ Microbiol 74(21):6720–6729. doi:10.1128/AEM.00968-08

Vignais PM, Colbeau A (2004) Molecular biology of microbial hydrogenases. Curr Issues Mol Biol 6:159–188

White D (2007) The physiology and biochemistry of prokaryotes, 3rd edn. Oxford University Press, New York

Willquist K, Zeidan AA, van Niel EW (2010) Physiological characteristics of the extreme thermophile *Caldicellulosiruptor saccharolyticus*: an efficient hydrogen cell factory. Microb Cell Factories 9:89. doi:10.1186/1475-2859-9-89

Yang SJ, Kataeva I, Hamilton-Brehm SD, Engle NL, Tschaplinske TJ, Doeppke C, Davis M, Wespheling J, Adams MW (2009) Efficient degradation of lignocellulosic plant biomass, without pretreatment, by the thermophilic anaerobe "*Anaerocellum thermophilum*" DSM 6725. Appl Environ Microbiol 75(14):4762–4769. doi:10.1128/AEM.00236-09